

## Probing of atomic beams by using a self-referencing principle

Stefan H. Kienle, Dietmar G. Fischer, and Matthias Freyberger  
*Abteilung für Quantenphysik, Universität Ulm, D-89069 Ulm, Germany*  
 (Received 31 August 1998)

We discuss a method for reconstructing the wave function of an atomic beam with the help of a self-referencing principle. At the heart of the method lies the controlled superposition of the original atomic matter wave with a single reference wave. For this purpose, Bragg scattering of atomic beams at standing light fields turns out to be perfectly suited. [S1050-2947(99)01508-5]

PACS number(s): 03.75.Be, 03.75.Dg

### I. INTRODUCTION

Coherent manipulation and coherent control of wavelike objects is certainly one of the most fascinating issues that reaches from classical physics to quantum physics. Concerning classical optics, the advent of the laser in 1960 has been the breakthrough to realize a striking application of coherent waves: *holography* [1] conceived by Gabor already in 1949. But holograms are by no means limited to recording interference patterns produced by classical light.

Early attempts have been made to apply the holographic principle to electron beams [2]. The further development of coherent electron sources has nowadays made electron holography a practical tool to study a wide range of topics ranging from very fundamental questions like the Aharonov-Bohm effect or the Sagnac effect for electron waves to high-resolution measurement at atomic dimensions [3].

Similarly, interferometry with neutron waves has become a powerful technique to perform many basic quantum experiments [4]. Also here the basic idea is to separate and to overlap the matter waves coherently, i.e., the holographic principle is indeed applied. This has been made possible by the use of perfect crystal interferometers which provide the coherent manipulation of the neutron beam [5].

Finally, atom interferometers [6] have proven to be perfect tools for fundamental studies in which the coherence properties of an atomic matter wave play an essential role. In particular, the mechanical effects of light on atoms [7] can be used to coherently split and recombine atom waves [8] in an extremely elegant way. In this realm of matter-wave interferometry the subjects studied range from fundamental, such as interferometer-based gravimeters [9] or wave-particle duality [10], to quite applied, such as nanostructuring [11].

This quantum-interference variety is based on one common and simple rule: the superposition principle for quantum states. This also provides the link to the classic holographic principle which basically relies on the coherent superposition of an object wave with an appropriate reference wave in order to store intensity and phase information of the object in the corresponding interferograms. As a consequence, the object can be reconstructed from suitable interference pictures.

These concepts turn out to be just as fruitful for the reconstruction of quantum states [12] which encode the complete knowledge of a quantum object. This has been demonstrated recently for the holographic reconstruction of molecular wave packets [13] and electronic Rydberg wave packets [14,15].

In the present work we are guided by the superposition principle in order to reconstruct the wave function of an atomic beam [16,17]. The basic question to be solved then is the suitable design of a reference wave function. In contrast to Refs. [13–15], we propose self-referencing [18], i.e., we superpose the object wave function with a replica of itself. This can be achieved with the help of Bragg scattering [19] of the atomic beam and we shall analyze the corresponding setup.

The paper is organized as follows. In Sec. II we discuss the heuristics of the proposed self-referencing principle for atom beams. For detailed calculations we refer the reader to Appendix A. The algorithm for evaluating the interferograms is explained in Sec. III and we illustrate the method with an example in Sec. IV. Finally, we conclude the paper with Sec. V.

### II. SELF-REFERENCING PRINCIPLE

Coherent superposition is a fundamental concept to handle information in wave physics [1]. It allows one to store and to retrieve amplitude *and* phase of a wavelike object. The key feature is interference of an object wave with a well-defined reference wave. The resulting interference pattern encodes the full information on amplitude and phase of the object.

We shall show how this principle can be applied to object waves that describe the quantum motion of atoms in a beam. In complete analogy to classical optics, the object matter wave to be analyzed interferes with a reference wave. The basic question is the proper design of this reference, which has to be added coherently to the object. We discuss a solution which uses a replica of the object as reference, i.e., we apply a self-referencing principle.

The quantum object to be measured in our case is a stationary beam of two-level atoms of mass  $m$  whose quantum motion at  $z=0$  is described by the state

$$|\Psi(x, z=0, t)\rangle = e^{-i(E/\hbar)t} \psi(x, z=0) |g\rangle \quad (1)$$

with the total energy  $E \equiv P^2/(2m)$  and with the internal ground state  $|g\rangle$ . To be more specific, we shall be concerned with the reconstruction of the wave function

$$\psi(x) \equiv \psi(x, z=0) = \frac{1}{\sqrt{2\pi\hbar}} \int_{-\infty}^{\infty} dp e^{ipx/\hbar} \tilde{\psi}(p) \quad (2)$$

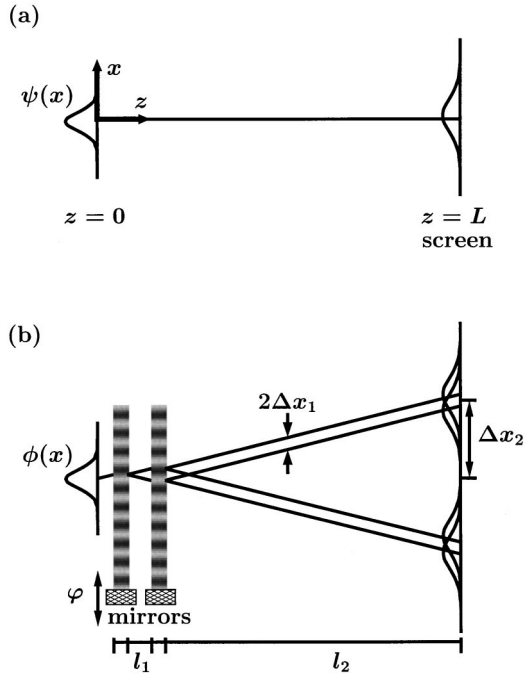


FIG. 1. Original atomic beam and the setup for the proposed self-referencing reconstruction. In (a) we illustrate the original beam of ground-state atoms described by a transverse wave function  $\psi(x)$  at  $z=0$ . Free evolution over the distance  $L$  simply broadens this wave function and we detect a smeared-out atomic position distribution at  $z=L$ . In (b) the original beam is tilted with respect to the two standing light fields. The corresponding wave function  $\phi(x) = e^{ikx}\psi(x)$  has an additional momentum shift of  $+\hbar k$ . Therefore, the dispersive interaction of the two-level atoms with the first standing laser field leads to Bragg scattering. This splits the atomic matter wave in two partial waves that are shifted by  $2\Delta x_1$ , Eq. (6), before they enter the second standing light field. Note that the size of the splitting depends on the distance  $l_1$ . Both partial waves undergo a second Bragg scattering process in the second field. On the screen at  $z=L$  the four partial waves overlap by pairs, provided the free evolution distance of length  $l_2$  is sufficiently large. Two position distributions  $w_\varphi(x, \Delta x_1)$  for two phases  $\varphi$  of the first standing light field are sufficient to unravel the essential information of the wave function  $\psi(x)$ : the *phase information*.

defining the transverse motion of the atom as indicated in Fig. 1(a). We assume the momentum amplitude  $\tilde{\psi}(p)$  to be well-concentrated around  $p=0$ .

How can we generate a reference signal that adds coherently to the object wave function  $\psi(x)$ ? The answer to this question is fairly simple: Let us use an atomic beam splitter [8] that divides the beam into two spatially separate but still coherent parts. After the beam splitter, the two partial waves can therefore interfere and the corresponding interference pattern, which in our case will be an atomic position distribution, does certainly contain information on amplitude and phase of  $\psi(x)$ . In the following we shall describe a concrete setup that allows us to measure interference patterns encoding even the *complete* information on amplitude and phase of  $\psi(x)$ .

Atomic beam splitting can be achieved with the help of Bragg scattering at a classical standing light field [8]. Thereby, the interaction of atom and field can be purely dispersive, that is, the frequency of the field is far detuned from

any atomic transition and the atom therefore remains in the ground state  $|g\rangle$ .

An appropriate scheme is depicted in Fig. 1(b). It consists of only a few basic elements: Two classical standing light fields of wave vector  $k$  scatter the atoms of the incoming beam in the interaction regions  $0 \leq z \leq z_0$  and  $z_0 + l_1 \leq z \leq 2z_0 + l_1$ , respectively. The sine-mode structure of the first field can be shifted relative to the second field in the  $x$  direction with the help of a moving mirror. The last element of our scheme is a screen at  $z=L \equiv 2z_0 + l_1 + l_2$ , where positions of scattered atoms are detected.

In the dispersive regime, the coupling constant  $\kappa$  of atom and field is small compared to the detuning  $\Delta$  and the interaction with each field is governed by the Hamiltonian [7]

$$\hat{H} = \frac{1}{2m} (\hat{p}^2 + \hat{p}_z^2) + \hbar \frac{\kappa^2}{\Delta} \sin^2(k\hat{x} + \varphi) \hat{\sigma}_3, \quad (3)$$

with the momentum operators  $\hat{p}$  and  $\hat{p}_z$  for the  $x$  and  $z$  directions. Internally, the spinlike operator  $\hat{\sigma}_3$  just leads to a phase change, i.e.,  $\hat{\sigma}_3|g\rangle = -|g\rangle$ . Hence due to the sinusoidal mode function the atoms do actually feel a periodic optical potential which leads to Bragg scattering of the atomic matter wave [19]. Furthermore, it is important to note that the relative position of the first periodic light structure is controlled via the phase  $\varphi$ , whereas for the second we simply have  $\varphi \equiv 0$ .

For a complete analysis of the scattering process in terms of wave functions, we refer the reader to Appendix A. Here we shall concentrate on the basic principles in order to bring out the idea.

We only get a Bragg resonance if the incoming atomic matter wave has a nonvanishing momentum component at  $p = \hbar k$ . This is just the same situation as encountered in scattering light from a perfect crystal. Since the momentum amplitude  $\tilde{\psi}(p)$ , Eq. (2), of our original atomic beam is concentrated around  $p=0$ , we have to shift it by  $\hbar k$  with respect to the first standing light field. This can be achieved by tilting the beam appropriately. In effect, the tilted beam can now be described by the shifted momentum amplitude

$$\tilde{\phi}(p) \equiv \tilde{\psi}(p - \hbar k), \quad (4)$$

which is peaked at  $p = \hbar k$ .

We emphasize that in order to create a shifted replica of the wave function, Eq. (2), by Bragg scattering, the momentum amplitude  $\tilde{\psi}(p)$  has to be narrow compared to a single photon momentum  $\hbar k$ . This means  $p/(\hbar k) \ll 1$  for all momenta with nonvanishing amplitude  $\tilde{\psi}(p)$ . In fact, this is the main limitation of our scheme.

As indicated in Fig. 1(b), the tilted atomic beam passes the first interaction zone with a specific probability without being deflected. For an appropriately long interaction time  $\tau_0$ , namely  $\tau_0 \gg \omega_r^{-1}$  with the photon recoil frequency  $\omega_r = \hbar k^2/(2m)$ , we will, however, also see a Bragg-resonance peak shifted by  $-2\hbar k$  from the incoming beam. Hence the momentum amplitude of the Bragg-scattered wave is located at  $p = -\hbar k$ . This coherent scattering process is fully governed by the Hamiltonian, Eq. (3), as shown in Appendix A.

The resulting atomic matter wave after the interaction zone therefore consists of two partial waves: a transmitted one and a reflected one.

It turns out that it is most convenient to describe this situation in terms of wave functions of the originally untilted atomic beam shown in Fig. 1(a). The transmitted wave after the first interaction zone is then effectively produced from such a virtual beam impinging orthogonally on the standing light field by kicking part of the atoms with a single photon momentum  $\hbar k$  in the  $+x$  direction, whereas the Bragg beam comes from the remaining part kicked by  $\hbar k$  in the  $-x$  direction. Both processes have to be weighted with certain probability amplitudes and their coherent sum describes the transmitted matter wave at  $z=z_0$ . From there on the atoms just experience free evolution over a distance  $l_1$ .

Putting these arguments together, we find for the state [20]

$$|\Phi(x, z=z_0+l_1, t)\rangle = e^{-i(E/\hbar)t} \phi(x, z=z_0+l_1) |g\rangle \quad (5)$$

of the matter wave at  $z=z_0+l_1$  a position amplitude

$$\begin{aligned} \phi(x, z_0+l_1) = e^{i\alpha_1} [C e^{ikx} \psi_{t_1}(x-\Delta x_1) - iS e^{-ikx} \\ \times e^{-2i\varphi} \psi_{t_1}(x+\Delta x_1)]. \end{aligned} \quad (6)$$

This expression reflects what we have said before. Its basic component is the wave function

$$\psi_{t_1}(x) = \frac{1}{\sqrt{2\pi\hbar}} \int_{-\infty}^{\infty} dp e^{-ip^2/(2m\hbar)t} \tilde{\psi}(p) e^{ipx/\hbar}, \quad (7)$$

which we obtain if the original  $\psi(x)$ , Eq. (2), evolves in free space for the time  $t=t_1 \equiv m(z_0+l_1)/P$ . That is,  $t_1$  is simply determined by the length  $z_0+l_1$  and by the known characteristic energy  $E \equiv P^2/(2m) \equiv \frac{1}{2}m v^2$  of the stationary atom beam.

Furthermore, the position amplitude, Eq. (6), is indeed a superposition of two copies of  $\psi_{t_1}$  weighted with the scattering amplitudes  $C = \cos[\kappa^2 z_0/(4\Delta v)]$  and  $S = \sin[\kappa^2 z_0/(4\Delta v)]$ , which we derive in Appendix A. Please note that the two partial waves of Eq. (6) are shifted by the spatial ruler

$$\Delta x_1 \equiv \frac{\hbar k}{P} l_1. \quad (8)$$

This is the essential parameter of the method which, as we will discuss below, limits the resolution of the reconstruction. In addition,  $\Delta x_1$  has a simple geometrical meaning since it is the displacement of a classical particle kicked by  $\hbar k$  and moving over a distance  $l_1$  with constant momentum  $P$ . Hence we can control  $\Delta x_1$  by changing  $l_1$ . The single photon kicks also lead to the phase factors  $e^{\pm ikx}$  in Eq. (6). Finally, we emphasize that the phase  $e^{-2i\varphi}$  of the superposition, Eq. (6), depends on the relative position of the first standing light field which can be varied by moving the mirror, as indicated in Fig. 1(b). The overall phase  $e^{i\alpha_1}$ , also derived in Appendix A, plays no role for our further considerations.

Therefore, we now understand the basic components of the position amplitude, Eq. (6). It would lead, of course, to

interferences in the atomic position distribution and these interferences originate from the superposition of  $\psi_{t_1}$  with an identical but shifted replica of itself. Hence the self-referencing principle becomes already visible in Eq. (6).

However, the corresponding interferograms would be very difficult to detect since they are dominated by the fast oscillations originating from the exponentials  $e^{\pm ikx}$ . Nevertheless, we emphasize that from a principle point of view interferograms taken at  $z_0+l_1$  would be sufficient to reconstruct the original wave function  $\psi(x)$ . But there is a way to get rid of these oscillations. We discuss this in the next section.

### Avoiding fast oscillations in the interferograms

Our aim is to construct interferograms which are determined by a superposition of the structure of Eq. (6), but without the fast oscillating phase factors  $e^{\pm ikx}$ .

For this purpose we first add a second interaction zone in the interval  $z_0+l_1 < z \leq 2z_0+l_1$  consisting of a standing light field identical to the first one. The Hamiltonian Eq. (3) again governs this interaction, but now for  $\varphi \equiv 0$ . Second, we add a further period of free evolution over the distance  $l_2$  until the atoms reach the screen at  $z=L \equiv 2z_0+l_1+l_2$ .

In complete analogy to the first scattering process, effectively described by Eq. (6), we now get a transformation of  $\phi(x, z_0+l_1)$ . Note that  $\phi(x, z_0+l_1)$  consists of two amplitudes  $e^{ikx} \psi_{t_1}(x-\Delta x_1)$  and  $e^{-ikx} \psi_{t_1}(x+\Delta x_1)$ , respectively. The corresponding momentum amplitude of the partial wave  $e^{ikx} \psi_{t_1}(x-\Delta x_1)$  is again centered at  $+\hbar k$  and hence the analysis of Appendix A can be applied immediately to find the transformation

$$\begin{aligned} e^{ikx} \psi_{t_1}(x-\Delta x_1) \rightarrow e^{i\alpha_2} [C e^{ikx} \psi_T(x-\Delta x_1-\Delta x_2) \\ - iS e^{-ikx} \psi_T(x-\Delta x_1+\Delta x_2)] \end{aligned} \quad (9)$$

in perfect analogy with Eq. (6). Here we have now used the abbreviations  $T = t_1 + t_2 = mL/P$  for the total evolution time and

$$\Delta x_2 \equiv \frac{\hbar k}{P} l_2 \quad (10)$$

reflecting the shift of the partial waves due to virtual momentum kicks. The overall phase  $e^{i\alpha_2}$ , appearing in Eq. (9), again plays no role for our considerations.

On the other hand, we can also apply the calculations of Appendix A to find the corresponding transformation of the partial amplitude  $e^{-ikx} \psi_{t_1}(x+\Delta x_1)$  which appears in Eq. (6) with its corresponding momentum amplitude centered at  $-\hbar k$ . We just replace  $k$  by  $-k$  in Eq. (9) and arrive at

$$\begin{aligned} e^{-ikx} \psi_{t_1}(x+\Delta x_1) \rightarrow e^{i\alpha_2} [C e^{-ikx} \psi_T(x+\Delta x_1+\Delta x_2) \\ - iS e^{ikx} \psi_T(x+\Delta x_1-\Delta x_2)]. \end{aligned} \quad (11)$$

With the help of Eqs. (9) and (11), we eventually understand the complete transformation of  $\phi(x, z_0+l_1)$ , Eq. (6), into the position amplitude

$$\begin{aligned}
\phi(x, L) = & e^{i(\alpha_1 + \alpha_2)} [C^2 e^{ikx} \psi_T(x - \Delta x_2 - \Delta x_1) \\
& - iCS e^{-ikx} \psi_T(x + \Delta x_2 - \Delta x_1) \\
& - iSC e^{-2i\varphi} e^{-ikx} \psi_T(x + \Delta x_2 + \Delta x_1) \\
& - S^2 e^{-2i\varphi} e^{ikx} \psi_T(x - \Delta x_2 + \Delta x_1)] \quad (12)
\end{aligned}$$

that describes the atomic matter wave in the plane  $z=L$ , i.e., on the detection screen.

We emphasize that the position amplitude, Eq. (12), basically consists of four replicas of the original wave function  $\psi(x)$  spread in free space for time  $T$  to give  $\psi_T(x)$ , as defined by Eq. (7). In principle, all four replicas contribute to a

$$w_\varphi(x, \Delta x_1) = |\phi(x, L)|^2 = \begin{cases} |C^2 \psi_T(x - \Delta x_2 - \Delta x_1) - e^{-2i\varphi} S^2 \psi_T(x - \Delta x_2 + \Delta x_1)|^2 & \text{for } x \geq 0 \\ (CS)^2 |\psi_T(x + \Delta x_2 - \Delta x_1) + e^{-2i\varphi} \psi_T(x + \Delta x_2 + \Delta x_1)|^2 & \text{for } x < 0 \end{cases} \quad (13)$$

now consists of two spatially separated parts [21]. The interferogram, Eq. (13), still depends on the phase  $\varphi$ , i.e., on the mirror position, and on the ruler  $\Delta x_1$ , Eq. (8). Both quantities are essential for analyzing the interferogram, as we point out in the next section, and they are both controlled by geometrical means.

We stress that Eq. (13) indeed constitutes the heart of our idea. It clearly shows again the self-referencing principle, namely the coherent superposition of  $\psi_T$  (object) with a shifted replica (reference). In addition, the interferograms are only determined by object wave and reference wave and we got rid of the fast oscillations complicating the scheme. The resulting interferences will allow us to reconstruct  $\psi_T(x)$  and eventually  $\psi(x)$ . We discuss the corresponding algorithm in the next section.

### III. EVALUATING THE INTERFERENCE DATA

It remains to be shown that the corresponding interferogram, Eq. (13), contains enough information to reconstruct the underlying wave function  $\psi_T(x)$ , Eq. (7). Eventually it is a straightforward task to find the desired  $\psi(x)$  by just inverting free time evolution.

We begin the evaluation of the interference data with a premeasurement of an atomic position distribution at  $z=L$ , where the light fields have been switched off. The resulting position distribution directly provides us the modulus  $|\psi_T(x)|$  and we can therefore focus on the reconstruction of the phase  $\Theta_T(x)$  of the wave function  $\psi_T(x) = |\psi_T(x)| \exp[i\Theta_T(x)]$ .

In the next step we measure two different distributions  $w_\varphi$ , Eq. (13), for the phases  $\varphi=0$  and  $\pi/4$ . We get the highest visibility for the interference patterns when we choose the scattering amplitudes  $C=S=1/\sqrt{2}$ . Then the appropriate combination

$$\begin{aligned}
w_0(x - \Delta x_2, \Delta x_1) - w_0(x + \Delta x_2, \Delta x_1) + i w_{\pi/4}(x + \Delta x_2, \Delta x_1) \\
- i w_{\pi/4}(x - \Delta x_2, \Delta x_1) = \psi_T(x - \Delta x_1) \psi_T^*(x + \Delta x_1) \quad (14)
\end{aligned}$$

position distribution measured on the screen at  $z=L$ . This is, however, not what we aim at. We want only two partial waves at a time to interfere with each other, namely those multiplied with either the  $e^{ikx}$  phase factor or the  $e^{-ikx}$  phase factor. Only in this case can we get rid of the fast oscillations in a position distribution dominated by  $e^{\pm ikx}$ .

We achieve such interferences by pairs, if the shift  $\Delta x_2$  becomes large enough so that the amplitudes  $\psi_T(x - \Delta x_2 \pm \Delta x_1)$  and  $\psi_T(x + \Delta x_2 \pm \Delta x_1)$  no longer overlap. Note further that  $\Delta x_2$ , Eq. (10), can be controlled simply by varying the distance  $l_2$ . Such a situation of overlap by pairs is indicated in Fig. 1(b) and the corresponding position distribution

does allow us to extract the pure interference term  $\psi_T(x - \Delta x_1) \psi_T^*(x + \Delta x_1)$ . We emphasize that the real part and the imaginary part of this interference term stem from two distinct interferograms recorded with  $\varphi=0$  and  $\varphi=\pi/4$ , respectively. We basically just subtract from each other the two spatially separated parts of one interferogram. Note further that the left-hand side of Eq. (14) contains only experimentally measurable distributions and known parameters of the setup.

Hence it remains to be shown how one can extract the phase  $\Theta_T$  from the interference term. From the premeasurement we know the modulus  $|\psi_T(x)|$  that allows us to determine the interval  $[x_{\min}, x_{\max}]$  in which  $\psi_T(x)$  differs substantially from zero. Now we start at the position  $x_{\min} + \Delta x_1$ . With the help of the interference term, Eq. (14), we evaluate the phase difference  $\Theta_T(x_{\min}) - \Theta_T(x_{\min} + 2\Delta x_1)$ . Proceeding to the point  $x_{\min} + 3\Delta x_1$ , we get  $\Theta_T(x_{\min} + 2\Delta x_1) - \Theta_T(x_{\min} + 4\Delta x_1)$ . In this way we go on to cover the complete interval  $[x_{\min}, x_{\max}]$  and to find the corresponding phase differences. In order to reconstruct the individual phases, we replace  $\Theta_T(x_{\min})$ , remaining unknown, by  $\Theta_T^{(\text{rec})}(x_{\min}) \equiv 0$ . With this initial phase setting we finally find recursively  $\Theta_T^{(\text{rec})}(x_{\min} + 2\Delta x_1)$ ,  $\Theta_T^{(\text{rec})}(x_{\min} + 4\Delta x_1)$ , ... from the phase differences.

Therefore, by evaluating the interference term, Eq. (14), in the way just described, we arrive at the reconstructed wave function

$$\psi_T^{(\text{rec})}(x) = \psi_T(x) e^{-i\Theta_T(x_{\min})}, \quad (15)$$

which is given on a grid with spacing  $2\Delta x_1$  in the interval  $[x_{\min}, x_{\max}]$ . Hence the parameter  $\Delta x_1$ , Eq. (8), defines the resolution of the method. The overall phase factor  $\exp[-i\Theta_T(x_{\min})]$  just expresses the well-known fact that any wave function is defined up to a constant phase. It is, however, worth noting that here such a phase comes in very naturally via the recursive algorithm.

As the final step, provided the resolution is sufficient, we can numerically propagate  $\psi_T^{(\text{rec})}$ , Eq. (15), back in time us-

ing Eq. (7), which eventually yields the reconstructed wave function

$$\psi^{(\text{rec})}(x) \cong \psi(x) e^{-i\Theta_T(x_{\text{min}})}. \quad (16)$$

Here the notation  $\cong$  reminds us that the reconstruction is, of course, limited by the resolution  $2\Delta x_1$  [22]. In the next section we shall discuss a numerical example that basically demonstrates the influence of the grid spacing  $2\Delta x_1$ .

#### IV. EXAMPLE

This section addresses two different topics. (i) First, we shall numerically show that the approximations made in the derivation of the Bragg scattered amplitudes, Eq. (6), are valid if the original atomic wave function  $\psi(x)$  is narrowly peaked in momentum space at  $p=0$ . (ii) Second, we shall illustrate the presented method for an example. In particular, we emphasize the influence of the resolution  $2\Delta x_1$ , which has a strong influence on the quality of the reconstructed matter wave.

##### A. Numerical check

Note that it is absolutely crucial for the presented method to have an analytical result at hand. Otherwise it would not have been possible to evaluate the interference data as shown in the preceding section. Since, on the other hand, the derivation of the Bragg scattered wave, Eq. (6), required several approximations, as shown in Appendix A, we now numerically check their validity.

For that purpose we use the wave function

$$\psi(x) = \mathcal{N} \left\{ \exp\left(-\frac{(x-x_0)^2}{2\sigma^2}\right) + i \exp\left(-\frac{(x+x_0)^2}{2\sigma^2}\right) \right\}, \quad (17)$$

which represents the atomic beam at  $z=0$  with parameters  $k\sigma=50$ ,  $kx_0=100$ , and a normalization constant  $\mathcal{N}$ . This Schrödinger-cat state is a superposition of two Gaussians centered at  $\pm x_0$  having the same width  $\sigma$ .

In Fig. 2(a), we depict the momentum distribution  $|\tilde{\phi}(p)|^2 = |\tilde{\psi}(p - \hbar k)|^2$  of the corresponding tilted beam. Note that it is peaked at  $p = +\hbar k$ . In Fig. 2(b), we show the momentum distribution after a single atom-field interaction calculated via the analytical expression, Eq. (6), for the scattered wave. Note that Fig. 2(b) coincides extremely well with the momentum distribution shown in Fig. 2(c), which we have obtained by numerically integrating Eq. (A10). The following parameters for atom, light field, and their interaction have been chosen:  $kz_0 = 5 \times 10^4$ ,  $P/(\hbar k) = 10^4$ , and  $\kappa^2 \tau_0 / (4\Delta) = \pi/4$ .

Also the overlap

$$\langle \Phi_{\text{ana}}(z_0) | \Phi_{\text{num}}(z_0) \rangle \approx 0.99 \quad (18)$$

between the analytical result and the numerical result for the scattered wave is very close to 1. This confirms the approximations made in Appendix A in order to get the analytical expression, Eq. (6), for the Bragg scattered wave. We emphasize that indeed the momentum distribution after the scattering process, see Figs. 2(b) and 2(c), has been splitted into

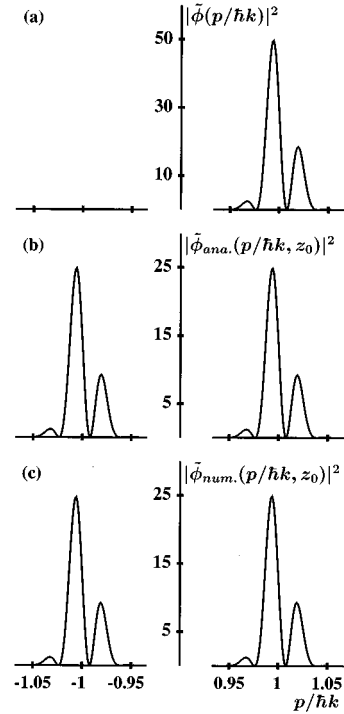


FIG. 2. Analytical result vs numerical simulation. In order to check Eq. (6) describing the Bragg scattering process, we compare it to the numerically integrated Schrödinger equation (A10). For this check the underlying state  $\psi(x)$  is a Schrödinger-cat state, Eq. (17). It is a superposition of two Gaussians of width  $k\sigma=50$ , spatially separated by  $2kx_0=200$ . The momentum distribution  $|\tilde{\phi}(p)|^2$  of the corresponding tilted beam described by  $\phi(x) = e^{ikx}\psi(x)$  is depicted in (a). Note that it is well-centered around  $p = \hbar k$ . The parameters of atom, field, and interaction have been chosen as follows:  $kz_0 = 5 \times 10^4$ ,  $P/(\hbar k) = 10^4$ , and  $\kappa^2 \tau_0 / (4\Delta) = \pi/4$ . After the interaction, the momentum distribution (b) calculated analytically with the help of Eq. (6) and the momentum distribution (c) calculated numerically with the help of Eq. (A10) are in perfect agreement.

two parts. One looks like the original and the other one—the replica—kept the shape but is shifted in momentum space from  $+\hbar k$  to  $-\hbar k$ .

##### B. Example for the reconstruction

To illustrate the reconstruction utilizing the self-referencing principle described in the previous sections, we use the Schrödinger-cat state of Eq. (17). For all parameters that define the atom, the standing light fields, and the corresponding interaction, we have chosen the same values as in the numerical simulation presented above.

Figure 3 shows the atomic position distributions  $w_\varphi$ —the interferograms—with  $k\Delta x_1 = 30$ ,  $k\Delta x_2 = 300$ , and field phases  $\varphi = 0$  and  $\varphi = \pi/4$ , respectively. These are the two required distributions  $w_0(x, \Delta x_1)$  and  $w_{\pi/4}(x, \Delta x_1)$  in order to apply the recursive reconstruction algorithm described in Sec. III.

With the help of these data, we have reconstructed the wave function  $\psi^{(\text{rec})}(x)$ , Eq. (16). The corresponding Wigner function is depicted in Fig. 4(b) and it agrees well with the Wigner function for the original matter wave  $\psi(x)$ , see Fig. 4(a).

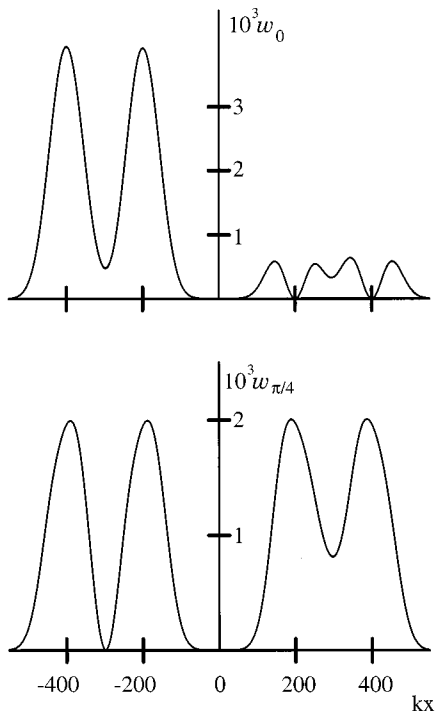


FIG. 3. Atomic position distributions  $w_\varphi(x, \Delta x_1)$ , Eq. (13), for the Schrödinger-cat state, Eq. (17), depicted for the two phases  $\varphi = 0$  and  $\varphi = \pi/4$  of the first standing light field. For the spatial ruler  $\Delta x_1$ , Eq. (8), and the separation  $\Delta x_2$ , Eq. (10), we have chosen the values  $k\Delta x_1 = 30$  and  $k\Delta x_2 = 300$ . All other parameters are the same as in Fig. 2. The spatial separation of the two parts of the position distributions caused by the free evolution after the second laser field and encoded in the parameter  $\Delta x_2$  is clearly visible. Note that according to Eq. (14) the distribution  $w_0$  yields the real part, whereas  $w_{\pi/4}$  yields the imaginary part of the interference term  $\psi_T(x - \Delta x_1)\psi_T^*(x + \Delta x_1)$ .

Figure 4(c) shows the same plot as 4(b) but for a spatial ruler  $k\Delta x_1 = 60$ . That is, we have a spatial resolution which is lower as in the reconstruction procedure for 4(b). Consequently, the reconstruction gets worse.

From this example, we see that the simple reconstruction algorithm based on Eq. (14) indeed works very well.

## V. CONCLUSIONS

We have discussed the reconstruction of wave functions describing the state of a stationary atomic beam. The method relies on a superposition principle: The object wave function interferes with a suited reference wave function. We have shown that only three interferograms are sufficient to retrieve the object wave function. The corresponding recursive algorithm has turned out to be quite simple and we have applied it to the reconstruction of a Schrödinger-cat wave function.

The simplicity of the algorithm, i.e., the simple recursive mapping of the measured data onto the wave function, is the main difference compared to the successful tomographic reconstruction of atomic beams [16]. On the other hand we can apply the proposed method only for reconstructing pure states and for beams with a narrow momentum distribution (for a different regime, see Ref. [17]).

We emphasize that the recent experiment described in Ref. [10], although treating a different type of problem,

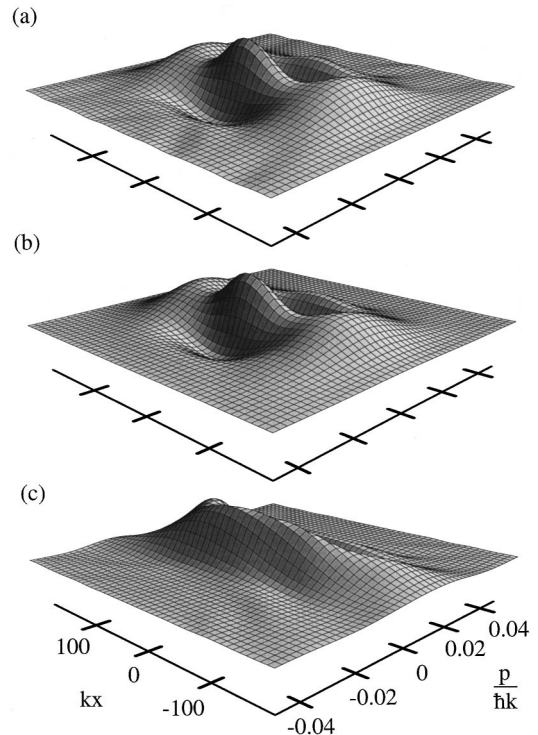


FIG. 4. Wigner functions of the initial wave function  $\psi(x)$  and the reconstructed wave functions  $\psi^{(\text{rec})}(x)$  exemplified here for the Schrödinger-cat state, Eq. (17). All Wigner functions have been plotted for the same parameters as in Fig. 2. In (a) we show the Wigner function of the initial Schrödinger-cat state, Eq. (17). The negative parts illustrate the nonclassical character of the state. (b) and (c) represent Wigner functions of the reconstructed wave functions  $\psi^{(\text{rec})}(x)$  for  $k\Delta x_2 = 300$  and two different values of the ruler  $k\Delta x_1$ , which sets the spatial resolution of our reconstruction scheme. In (b) we have used  $k\Delta x_1 = 30$  and the reconstructed Wigner function agrees very well with the initial one. However, as shown in (c), the reconstruction quality decreases when we increase the value to  $k\Delta x_1 = 60$ .

comes already very close to a possible realization of the idea analyzed in the present work. Furthermore, we are convinced that it would be very interesting to apply our reconstruction scheme to the cw output beam of an atom laser [23].

## ACKNOWLEDGMENTS

The authors thank V. P. Yakovlev, S.-Y. Zhu, and I. A. Walmsley for many fruitful and vivifying discussions and the DAAD for financial support. S. H. K. acknowledges support by the Studienstiftung des Deutschen Volkes.

## APPENDIX: SCATTERED ATOMIC MATTER WAVE

In this appendix we explicitly analyze the dispersive Bragg scattering of an atom beam at a standing light field. Since it is most appropriate for our purpose, we shall present the calculations in terms of wave functions. In fact, according to the setup shown in Fig. 1(b), we have to investigate two such scattering events. However, since the corresponding standing light fields are identical, we can simply use the analysis, described below, twice.

We start with a matter wave of two-level atoms described by the state

$$\begin{aligned} |\Psi(x, z=0, t)\rangle &= e^{-iEt/\hbar} |\psi(x, z=0)\rangle |g\rangle \\ &= e^{-iEt/\hbar} \frac{1}{\sqrt{2\pi\hbar}} \int_{-\infty}^{\infty} dp e^{ipx/\hbar} \tilde{\psi}(p, z=0) |g\rangle \end{aligned} \quad (\text{A1})$$

in the plane  $z=0$ . We assume the beam to be infinitely extended in the  $y$  direction. Here  $E$  denotes the total energy of the stationary state and the atoms have been prepared in their internal ground state  $|g\rangle$ . Our final aim is the reconstruction of the wave function  $\psi(x) \equiv \psi(x, z=0)$  or the corresponding momentum amplitude  $\tilde{\psi}(p) \equiv \tilde{\psi}(p, z=0)$ .

Note that  $\tilde{\psi}(p)$  of the original beam is well-concentrated around  $p=0$ . However, in order to get Bragg resonances we need an atomic beam with a momentum amplitude having nonvanishing contributions at  $p=\hbar k$  and hence we have to shift the original momentum amplitude by  $+\hbar k$ . This constant shift by  $\hbar k$  can be approximately achieved if the atomic beam impinges nonorthogonally on the standing light field, as indicated in Fig. 1(b). Hence in the calculations below, we will be concerned with a shifted amplitude  $\tilde{\phi}(p) \equiv \tilde{\psi}(p - \hbar k)$  describing atoms in the tilted beam in momentum representation.

The dispersive interaction between atoms and laser light in the region  $0 \leq z \leq z_0$  can be described by the Hamiltonian, Eq. (3),

$$\hat{H} = \frac{\hat{p}^2 + \hat{p}_z^2}{2m} + \hbar \frac{\kappa^2}{\Delta} \sin^2(k\hat{x} + \varphi) \hat{\sigma}_3. \quad (\text{A2})$$

To determine the stationary solution at  $z=z_0$ , we substitute the ansatz

$$\begin{aligned} |\Phi(x, z, t)\rangle &= e^{-iEt/\hbar} \phi(x, z) |g\rangle \\ &= e^{-iEt/\hbar} \frac{1}{\sqrt{2\pi\hbar}} \int_{-\infty}^{\infty} dp e^{i[p_z(p)z + px]/\hbar} \tilde{\phi}(p, z) |g\rangle \end{aligned} \quad (\text{A3})$$

in the time-dependent Schrödinger equation

$$i\hbar \frac{\partial}{\partial t} |\Phi\rangle = \hat{H} |\Phi\rangle, \quad (\text{A4})$$

where we can choose  $p_z(p)$  so that  $\tilde{\phi}(p, z)$  is a slowly varying amplitude. Then we arrive at the equation

$$\begin{aligned} \left( E + \hbar \frac{\kappa^2}{2\Delta} \right) \phi(x, z) &= \left[ \frac{\hat{p}^2 + \hat{p}_z^2}{2m} + \hbar \frac{\kappa^2}{2\Delta} \right. \\ &\quad \left. \times \cos 2(kx + \varphi) \right] \phi(x, z), \end{aligned} \quad (\text{A5})$$

which, using Eq. (A3), reads

$$\begin{aligned} &\left( E + \hbar \frac{\kappa^2}{2\Delta} - \frac{p^2 + p_z^2(p)}{2m} \right) e^{ip_z(p)z/\hbar} \tilde{\phi}(p, z) \\ &= e^{ip_z(p)z/\hbar} \left[ -i \frac{\hbar}{m} p_z(p) \frac{\partial}{\partial z} - \frac{\hbar^2}{2m} \frac{\partial^2}{\partial z^2} \right] \tilde{\phi}(p, z) \\ &\quad + \hbar \frac{\kappa^2 e^{-2i\varphi}}{4\Delta} e^{ip_z(p+2\hbar k)z/\hbar} \tilde{\phi}(p+2\hbar k, z) \\ &\quad + \hbar \frac{\kappa^2 e^{2i\varphi}}{4\Delta} e^{ip_z(p-2\hbar k)z/\hbar} \tilde{\phi}(p-2\hbar k, z) \end{aligned}$$

in momentum representation. Now we choose  $p_z(p)$  so that

$$\frac{p^2 + p_z^2(p)}{2m} = E \equiv \frac{P^2}{2m} \quad (\text{A6})$$

and we neglect the term  $\hbar \kappa^2/(2\Delta) \ll E$ . Furthermore, the total energy  $E$  is assumed to be much larger than any transversal kinetic energy  $p^2/(2m)$ . Hence the momentum in the  $z$  direction is basically dominated by  $p_z(p) \approx P$  and  $\tilde{\phi}(p, z)$  is slowly varying with  $z$ . Consequently, we neglect second derivatives

$$\left| \frac{\partial^2}{\partial z^2} \tilde{\phi}(p, z) \right| \ll \frac{2p_z(p)}{\hbar} \left| \frac{\partial}{\partial z} \tilde{\phi}(p, z) \right|, \quad (\text{A7})$$

which considerably simplifies Eq. (A6) and we find

$$\begin{aligned} i v \frac{\partial}{\partial z} \tilde{\phi}(p, z) &= \frac{\kappa^2 e^{-2i\varphi}}{4\Delta} e^{i[p_z(p+2\hbar k) - p_z(p)]z/\hbar} \tilde{\phi}(p+2\hbar k, z) \\ &\quad + \frac{\kappa^2 e^{2i\varphi}}{4\Delta} e^{i[p_z(p-2\hbar k) - p_z(p)]z/\hbar} \tilde{\phi}(p-2\hbar k, z), \end{aligned} \quad (\text{A8})$$

where we have introduced the characteristic velocity  $v \equiv P/m$ . Expanding

$$p_z(p) = \sqrt{P^2 - p^2} \approx P - p^2/(2P) \quad (\text{A9})$$

in the exponents of Eq. (A8) yields

$$\begin{aligned} i v \frac{\partial}{\partial z} \tilde{\phi}(p, z) &= \frac{\kappa^2 e^{-2i\varphi}}{4\Delta} e^{-2i(\hbar k + p)kz/P} \tilde{\phi}(p+2\hbar k, z) \\ &\quad + \frac{\kappa^2 e^{2i\varphi}}{4\Delta} e^{-2i(\hbar k - p)kz/P} \tilde{\phi}(p-2\hbar k, z). \end{aligned} \quad (\text{A10})$$

We solve this differential equation in the interaction region  $0 \leq z \leq z_0$  with the boundary condition  $\tilde{\phi}(p, 0) = \tilde{\phi}(p)$ .

Formally integrating Eq. (A10) leads to

$$i[\tilde{\phi}(p, z_0) - \tilde{\phi}(p)] = \frac{\kappa^2 e^{-2i\varphi}}{4\Delta v} \int_0^{z_0} dz e^{-2i(\hbar k + p)kz/P} \\ \times \tilde{\phi}(p + 2\hbar k, z) + \frac{\kappa^2 e^{2i\varphi}}{4\Delta v} \\ \times \int_0^{z_0} dz e^{-2i(\hbar k - p)kz/P} \tilde{\phi}(p - 2\hbar k, z). \quad (\text{A11})$$

Let us have a closer look at the integrals on the right-hand side. Since we assume  $\tilde{\phi}(p, z)$  to vary slowly with  $z$ , the behavior of the integrals is dominated by the exponential functions. We first consider momenta close to  $\hbar k$  that is  $2|\hbar k - p|kz_0/P < 1$ . Then the value of the first integral is determined by the fast oscillating exponential  $e^{-4i\hbar k^2 z/P} \equiv e^{-8i\omega_r z/v}$ , because we work in the Bragg regime defined by the first condition [7,19]

$$4\omega_r \tau_0 \gg 1, \quad (\text{A12})$$

where  $\omega_r = \hbar k^2/(2m)$  denotes the photon recoil frequency and  $\tau_0 \equiv z_0/v$  denotes the characteristic atom-light interaction time. We can now estimate the first integral by approximating  $\tilde{\phi}(p + 2\hbar k, z)$  with a constant of the order 1. Hence the value of the first integral is restricted by the factor  $v/(4\omega_r)$ , which finally means that due to the second Bragg condition [7,19]

$$\hbar \frac{\kappa^2}{4\Delta} \ll 4\hbar \omega_r \quad (\text{A13})$$

we can neglect the first term in Eq. (A11). The second Bragg condition forces the maximal optical potential seen by the atoms to be much weaker than the photon recoil energy. Analogously when  $p$  is close to  $-\hbar k$  the second integral vanishes.

The above reasoning allows us to rewrite Eq. (A11) in terms of two coupled equations

$$i v \frac{\partial}{\partial z} \tilde{\phi}(\varphi + \hbar k, z) = \frac{\kappa^2 e^{2i\varphi}}{4\Delta} e^{2i\varphi(kz/P)} \tilde{\phi}(\varphi - \hbar k, z) \quad (\text{A14})$$

for momenta close to  $\hbar k$ , i.e.,  $p = \varphi + \hbar k$ , and

$$i v \frac{\partial}{\partial z} \tilde{\phi}(\varphi - \hbar k, z) = \frac{\kappa^2 e^{-2i\varphi}}{4\Delta} e^{-2i\varphi(kz/P)} \tilde{\phi}(\varphi + \hbar k, z) \quad (\text{A15})$$

for momenta close to  $-\hbar k$ , i.e.,  $p = \varphi - \hbar k$ . In the following we denote by  $\varphi$  the small deviations from the photon momentum  $\pm \hbar k$  and we keep in mind that these deviations have to fulfill the condition

$$\frac{2|\hbar k \pm p|kz_0}{P} \equiv 4\omega_r \tau_0 \frac{|\varphi|}{\hbar k} < 1, \quad (\text{A16})$$

with the characteristic interaction time  $\tau_0 = z_0/v$ .

In order to solve the coupled differential equations (A14) and (A15), we differentiate them with respect to the  $z$  coordinate and find the uncoupled equations

$$\frac{\partial^2}{\partial z^2} \tilde{\phi}(\varphi \pm \hbar k, z) \mp 2i\varphi \frac{k}{P} \frac{\partial}{\partial z} \tilde{\phi}(\varphi \pm \hbar k, z) \\ + \left( \frac{\kappa^2}{4\Delta v} \right)^2 \tilde{\phi}(\varphi \pm \hbar k, z) = 0 \quad (\text{A17})$$

which are valid for  $\tilde{\phi}(\varphi + \hbar k, z)$  and  $\tilde{\phi}(\varphi - \hbar k, z)$ , respectively. The boundary conditions

$$\tilde{\phi}(\varphi \pm \hbar k, z=0) = \tilde{\phi}(\varphi \pm \hbar k) \quad (\text{A18})$$

and

$$\frac{\partial}{\partial z} \tilde{\phi}(\varphi \pm \hbar k, z=0) = -i \frac{\kappa^2 e^{\pm 2i\varphi}}{4\Delta v} \tilde{\phi}(\varphi \mp \hbar k) \quad (\text{A19})$$

are fixed by demanding that at  $z=0$  the solutions have to coincide with  $\tilde{\phi}(p)$ . As mentioned before, we concentrate on a situation where  $\tilde{\phi}(p)$  differs from zero only in the vicinity of  $p = \hbar k$ , that is, the tilted incident matter wave has a momentum distribution peaked at  $\hbar k$  and therefore  $\tilde{\phi}(\varphi - \hbar k) = 0$ .

With the ansatz

$$\tilde{\phi}(\varphi \pm \hbar k, z) = e^{\pm i\varphi(k/P)z} f(\varphi \pm \hbar k, z), \quad (\text{A20})$$

Eq. (A17) reduces to

$$\frac{\partial^2}{\partial z^2} f(\varphi \pm \hbar k, z) + \left( \frac{\kappa^2}{4\Delta v} \right)^2 f(\varphi \pm \hbar k, z) = 0 \quad (\text{A21})$$

when we neglect terms of the order  $\varphi(k/P)$  compared to those of the order  $\kappa^2/(4\Delta v)$ . Consequent application of this approximation leads us to the final expression for the scattered atomic matter wave

$$\tilde{\phi}(p, z) = \begin{cases} e^{i\varphi(k/P)z} \cos\left(\frac{\kappa^2 z}{4\Delta v}\right) \tilde{\phi}(\varphi + \hbar k) & \text{for } p = \varphi + \hbar k \\ -ie^{-2i\varphi} e^{-i\varphi(k/P)z} \sin\left(\frac{\kappa^2 z}{4\Delta v}\right) \tilde{\phi}(\varphi + \hbar k) & \text{for } p = \varphi - \hbar k. \end{cases} \quad (\text{A22})$$

Note that the momentum amplitude  $\tilde{\phi}(p, z)$  now has two coherent contributions: one part is centered around  $p = \hbar k$  and a second part is centered around  $p = -\hbar k$ . Both parts are determined by the original amplitude  $\tilde{\phi}(p)$  of the incoming beam and by the scattering amplitudes  $\cos[\kappa^2 z/(4\Delta v)]$  and  $\sin[\kappa^2 z/(4\Delta v)]$ . The phase factors  $\exp(\pm i(\varphi/P)kz)$  express the relative Doppler shift of the two coherent contributions of  $\tilde{\phi}(p, z)$ . Hence depending on the scattering length  $z$ , we basically have weighted replicas of the incoming momentum amplitude oscillating [24] between the centers at  $+\hbar k$  and  $-\hbar k$ , respectively. In addition, we can control their mutual phase relation via the factor  $\exp(-2i\varphi)$ . Equation (A22) clearly formulates the self-referencing principle: Due to the Bragg scattering of atoms at a standing light field, we get a second reference amplitude centered at  $p = -\hbar k$  phase coherently added to the incoming amplitude at  $p = +\hbar k$ .

Finally, we have to translate the momentum amplitude, Eq. (A22), back into position representation since eventually we will detect an atomic position distribution. Moreover, it will turn out that the atomic matter wave after the Bragg-scattering process can be written most nicely in terms of the original wave function  $\psi(x)$ , Eq. (A1), which describes the originally untilted beam.

In order to show this, we start from the position amplitude at  $z = z_0$  [Eq. (A3)], which reads

$$\phi(x, z = z_0) = \frac{1}{\sqrt{2\pi\hbar}} \int_{-\infty}^{\infty} dp e^{i[p_z(p)z_0 + px]/\hbar} \phi(p, z_0) \quad (\text{A23})$$

with the corresponding momentum amplitude  $\tilde{\phi}(p, z_0)$ , Eq. (A22). For positions  $z > z_0$  the interaction with the light field is now switched off, i.e.,  $\kappa = 0$  in the Hamiltonian, Eq. (A2). Hence in order to calculate the wave function at a point  $z > z_0$ , we simply repeat our considerations with a simple free Hamiltonian and with boundary conditions as set by Eq. (A22) and find

$$\begin{aligned} \phi(x, z > z_0) &= \frac{1}{\sqrt{2\pi\hbar}} \int_{-\infty}^{\infty} dp e^{i p_z(p)(z-z_0)/\hbar} \\ &\times e^{i[p_z(p)z_0 + px]/\hbar} \tilde{\phi}(p, z_0) \end{aligned} \quad (\text{A24})$$

with  $p_z(p) = \sqrt{2mE - p^2} = \sqrt{P^2 - p^2}$ . Substituting the momentum amplitude  $\tilde{\phi}(p, z_0)$ , Eq. (A22), and expanding  $p_z(p) \approx P - p^2/(2P)$  we finally arrive at

$$\begin{aligned} \phi(x, z_0 + l_1) &= e^{i\alpha_1} \left[ e^{ikx} \cos\left(\frac{\kappa^2 z_0}{4\Delta v}\right) \frac{1}{\sqrt{2\pi\hbar}} \right. \\ &\times \int_{-\infty}^{\infty} d\varphi e^{-i\varphi^2/(2\hbar P)(z_0 + l_1)} \\ &\times \tilde{\phi}(\hbar k + \varphi) e^{i[x - (\hbar k/P)l_1]\varphi/\hbar} \\ &- i e^{-2i\varphi} e^{-ikx} \sin\left(\frac{\kappa^2 z_0}{4\Delta v}\right) \frac{1}{\sqrt{2\pi\hbar}} \\ &\times \int_{-\infty}^{\infty} d\varphi e^{-i\varphi^2/(2\hbar P)(z_0 + l_1)} \\ &\left. \times \tilde{\phi}(\hbar k + \varphi) e^{i[x + (\hbar k/P)l_1]\varphi/\hbar} \right]. \end{aligned} \quad (\text{A25})$$

Here the overall phase  $\alpha_1 = [P/\hbar - \hbar k^2/(2P)](z_0 + l_1)$  is of no interest, since it will not affect any position distribution. Note that in Eq. (A25) we have extended the  $\varphi$  integration since the momentum amplitude  $\tilde{\phi}(\varphi + \hbar k) = \tilde{\psi}(\varphi)$  is centered around  $\varphi = 0$  and therefore automatically restricts the integration.

The essential features of the state, Eq. (A25), become much clearer when we rewrite it as

$$\begin{aligned} \phi(x, z_0 + l_1) &= e^{i\alpha_1} [C e^{ikx} \psi_{t_1}(x - \Delta x_1) \\ &- i S e^{-ikx} e^{-2i\varphi} \psi_{t_1}(x + \Delta x_1)] \end{aligned} \quad (\text{A26})$$

with the wave function

$$\begin{aligned} \psi_{t_1}(x) &= \frac{1}{\sqrt{2\pi\hbar}} \int_{-\infty}^{\infty} d\varphi e^{-i\varphi^2/(2m\hbar)t} \tilde{\phi}(\hbar k + \varphi) e^{i\varphi x/\hbar} \\ &= \frac{1}{\sqrt{2\pi\hbar}} \int_{-\infty}^{\infty} d\varphi e^{-i\varphi^2/(2m\hbar)t} \tilde{\psi}(\varphi) e^{i\varphi x/\hbar} \end{aligned} \quad (\text{A27})$$

evolving in free space over a time  $t = t_1 = m(z_0 + l_1)/P$ . The spatial ruler

$$\Delta x_1 = \frac{\hbar k}{P} l_1, \quad (\text{A28})$$

the scattering amplitudes

$$C = \cos\left(\frac{\kappa^2 z_0}{4\Delta v}\right) \quad (\text{A29})$$

and

$$S = \sin\left(\frac{\kappa^2 z_0}{4\Delta v}\right), \quad (\text{A30})$$

as well as the phase  $\varphi$  are the essential parameters defining the coherent superposition, Eq. (A26). We emphasize that the wave function defining this superposition is just a time-evolved replica of the one describing the originally untilted beam. The time  $t_1$ , basically defined by the distance  $l_1$  and therefore at our disposal, is the time a free classical particle

with kinetic energy  $E = P^2/(2m)$  would need to overcome this distance. Similarly, the ruler  $\Delta x_1$ , Eq. (A28), has a simple geometrical interpretation: It is the transverse shift a classical particle would accumulate over the distance  $l_1$  after being kicked by a photon momentum  $\hbar k$ . Equation (A26) as a whole therefore has an obvious geometrical interpretation and we can see how  $\psi_{t_1}(x)$  plays a twofold role in the proposed scheme: it is the object signal and the reference signal at the same time.

- 
- [1] D. Gabor, Proc. R. Soc. London, Ser. A **197**, 454 (1949).
- [2] M. E. Haine and T. Mulvey, J. Opt. Soc. Am. **42**, 763 (1952).
- [3] For an overview concerning modern electron holography, see A. Tonomura, Phys. Today **43** (4), 22 (1990).
- [4] See the intriguing work on wave-particle duality by H. Rauch and J. Summhammer, Phys. Lett. A **104**, 44 (1984) and the further analysis by D. M. Greenberger and A. Yasin, *ibid.* **128**, 391 (1988) and as a most recent example we also mention the observation of geometric and dynamical phases by neutron interferometry, B. E. Allmann, H. Kaiser, S. A. Werner, A. G. Wagh, V. C. Rakhecha, and J. Summhammer, Phys. Rev. A **56**, 4420 (1997).
- [5] For reviews on neutron interferometry we refer the reader to *Neutron Interferometry*, edited by U. Bonse and H. Rauch (Clarendon Press, Oxford, 1979); *Matter Wave Interferometry*, edited by G. Badurek, H. Rauch, and A. Zeilinger (North Holland, Amsterdam, 1988); H. Rauch, Contemp. Phys. **27**, 345 (1986); D. Greenberger, Rev. Mod. Phys. **55**, 875 (1983).
- [6] O. Carnal and J. Mlynek, Phys. Rev. Lett. **66**, 2689 (1991); D. W. Keith, C. R. Ekstrom, Q. A. Turchette, and D. E. Pritchard, *ibid.* **66**, 2693 (1991); C. J. Bordé, Phys. Lett. A **140**, 10 (1989); V. P. Chebotayev, B. Dubetsky, A. P. Kasantsev, and V. P. Yakovlev, J. Opt. Soc. Am. B **2**, 1791 (1985); F. Riehle, T. Kisters, A. White, J. Helmecke, and C. J. Bordé, Phys. Rev. Lett. **67**, 177 (1991); M. Kasevich and S. Chu, *ibid.* **67**, 181 (1991); U. Sterr, K. Sengstock, J. H. Müller, D. Bettermann, and W. Ertmer, Appl. Phys. B: Photophys. Laser Chem. **54**, 341 (1992); E. M. Rasel, M. K. Oberthaler, H. Batelaan, J. Schmiedmayer, and A. Zeilinger, Phys. Rev. Lett. **75**, 2633 (1995).
- [7] A. P. Kazantsev, G. I. Surdutovich, and V. P. Yakovlev, *Mechanical Action of Light on Atoms* (World Scientific, Singapore, 1990).
- [8] T. Sleator, T. Pfau, V. Balykin, O. Carnal, and J. Mlynek, Phys. Rev. Lett. **68**, 1996 (1992); T. Pfau, C. Kurtsiefer, C. S. Adams, M. Sigel, and J. Mlynek, *ibid.* **71**, 3427 (1993); R. Deutschmann, W. Ertmer, and H. Wallis, Phys. Rev. A **47**, 2169 (1993); D. M. Giltner, R. W. McGowan, and S. A. Lee, Phys. Rev. Lett. **75**, 2638 (1995); S. Choi, H. M. Wiseman, S. M. Tan, and D. F. Walls, Phys. Rev. A **55**, 527 (1997).
- [9] M. Kasevich and S. Chu, Appl. Phys. B: Photophys. Laser Chem. **54**, 321 (1992).
- [10] S. Dürr, T. Nonn, and G. Rempe, Nature (London) **395**, 33 (1998).
- [11] U. Drodofsky, J. Stuhler, Th. Schulze, M. Drewsen, B. Brezger, T. Pfau, and J. Mlynek, Appl. Phys. B: Lasers Opt. **65**, 755 (1997).
- [12] Special Issue of J. Mod. Opt. 44, no. 11 and 12 (1997) on *State Preparation and Measurement*, edited by W. P. Schleich and M. G. Raymer; D. Leibfried, T. Pfau, and C. Monroe, Phys. Today **51** (4), 22 (1998); M. Freyberger, P. J. Bardroff, C. Leichtle, G. Schrade, and W. P. Schleich, Phys. World **10** (11), 41 (1997); D.-G. Welsch, W. Vogel, T. Opatrny, *Progress in Optics XXXIX* (North-Holland, Amsterdam, 1998); U. Leonhardt, *Measuring the Quantum State of Light* (Cambridge University Press, Cambridge, 1997).
- [13] C. Leichtle, W. P. Schleich, I. Sh. Averbukh, and M. Shapiro, Phys. Rev. Lett. **80**, 1418 (1998).
- [14] T. C. Weinacht, J. Ahn, and P. H. Bucksbaum, Phys. Rev. Lett. **80**, 5508 (1998).
- [15] X. Chen and J. A. Yeazell, Phys. Rev. A **56**, 2316 (1997).
- [16] C. Kurtsiefer, T. Pfau, and J. Mlynek, Nature (London) **386**, 150 (1997); U. Janicke and M. Wilkens, J. Mod. Opt. **42**, 2183 (1995).
- [17] M. Freyberger, S. H. Kienle, and V. P. Yakovlev, Phys. Rev. A **56**, 195 (1997); S. H. Kienle, D. Fischer, W. P. Schleich, V. P. Yakovlev, and M. Freyberger, Appl. Phys. B: Lasers Opt. **65**, 735 (1997); I. A. Walmsley and N. P. Bigelow, Phys. Rev. A **57**, R713 (1998).
- [18] A self-referencing interferometric technique for measuring amplitude and phase of ultrashort optical pulses was given by C. Iaconis and I. A. Walmsley, Opt. Lett. **23**, 792 (1998).
- [19] E. Arimondo, A. Bambini, and S. Stenholm, Phys. Rev. A **24**, 898 (1981); A. F. Bernhardt and B. W. Shore, *ibid.* **23**, 1290 (1981); P. J. Martin, B. G. Oldaker, A. Miklich, and D. E. Pritchard, Phys. Rev. Lett. **60**, 515 (1988); S. Kunze, S. Dürr, and G. Rempe, Europhys. Lett. **34**, 343 (1996); S. Kunze, S. Dürr, K. Dieckmann, M. Elbs, U. Ernst, A. Hardell, S. Wolf, and G. Rempe, J. Mod. Opt. **44**, 1863 (1997); M. Marte and S. Stenholm, Appl. Phys. B: Photophys. Laser Chem. **54**, 443 (1992); M. Wilkens, E. Schumacher, and P. Meystre, Phys. Rev. A **44**, 3130 (1991).
- [20] Note that we denote wave functions of the tilted beam, which actually impinges on the light fields, by the symbols  $\Phi$  and  $\phi$ , respectively.
- [21] At this point we emphasize the need for quite a monochromatic beam, i.e.,  $\delta P/P$  has to be small. The evolution time  $T = mL/P$  as well as the shifts  $\Delta x_1 = \hbar k l_1/P$  and  $\Delta x_2 = \hbar k l_2/P$  will fluctuate with a nonmonochromatic beam and the interference information in Eq. (13) will be washed out eventually. Let  $\varphi$  denote the momentum width (see Appendix A) of the original wave function  $\psi(x)$ . Then the fluctuations  $\delta T = (mL/P)(\delta P/P)$  of the time  $T$  lead to fluctuations  $\varphi^2/(2m\hbar)\delta T$  in the dynamical phase of  $\psi_T$ . These fluctua-

tions have to be small, i.e.,  $\varphi^2 L / (2\hbar P) (\delta P / P) \ll 1$ . On the other hand, the fluctuations  $\delta(\Delta x_2)$  have to be much smaller than the characteristic width  $\hbar/\varphi$  of the atomic wave function, i.e.,  $(k\varphi l_2 / P) (\delta P / P) \ll 1$ . Since we have  $\varphi \ll \hbar k$  and  $l_2 \approx L$ , the latter inequality is crucial for the monochromaticity. For the example considered in Sec. IV, we have  $k\Delta x_2 = 300$  and  $\varphi / (\hbar k) \leq 1/10$  and we therefore need a monochromaticity  $\delta P / P < 5\%$ .

[22] Note that  $\psi^{(\text{m})}(x)$  can be calculated at any point  $x$ . Its accuracy, however, depends on the values of the wave function  $\psi_T^{(\text{rec})}(x)$  given only on a grid with spacing  $2\Delta x_1$ . The corresponding restriction can be seen most easily when we consider the numerical calculation of the momentum amplitude  $\tilde{\psi}_T(p)$ . The Fourier transform becomes a periodic Fourier sum and we have to restrict ourselves to momenta  $|p|/\hbar k \leq (2\Delta x_1 \pi/k)$ .

This is just another expression of the well-known Nyquist theorem (or sampling theorem). In other words, due to the fundamental position resolution given by  $2\Delta x_1$ , we can only resolve momenta up to  $\pm \pi\hbar/(2\Delta x_1)$ .

- [23] R. J. C. Spreeuw, T. Pfau, U. Janicke, and M. Wilkens, *Europhys. Lett.* **32**, 469 (1996); H. M. Wiseman, A. Martins, and D. F. Walls, *Quantum Semiclass. Opt.* **8**, 737 (1996); M. Holland, K. Burnett, C. W. Gardiner, J. I. Cirac, and P. Zoller, *Phys. Rev. A* **54**, R1757 (1996); M. Naraschewski, A. Schenzle, and H. Wallis, *ibid.* **56**, 603 (1997); O. Zobay and P. Meystre, *ibid.* **57**, 4710 (1998); B. Kneer, T. Wong, K. Vogel, W. P. Schleich, and D. F. Walls, *ibid.* **58**, 4841 (1998).
- [24] For the quantum Pendellösung, see P. Meystre, E. Schumacher, and E. M. Wright, *Ann. Phys. (Leipzig)* **48**, 141 (1991).